

Surface Temperature Inversion Analysis in Beijing Municipal Area

Weijia Wang *

Department of Earth, Atmosphere and Environment, Northern Illinois University, DeKalb, US

* Corresponding author: Z2046743@students.niu.edu

Abstract. The urban heat island (UHI) effect means the temperature in the city is significantly higher than that in the peripheral suburbs. It is important to research the UHI effect to understand how human activities affect the urban climate, supporting the reduction of pollution in the urban environment, controlling energy consumption, and improving urban residents' health. This study takes downtown Beijing as an example and uses Landsat 8 satellite data to analyze the surface temperature inversion by preprocessing the remote sensing images, such as radiometric calibration and atmospheric correction, combined with the vegetation index (NDVI) inversion, and using the surface thermal radiation intensity calculation and the single-window algorithm, to derive the distribution of the surface temperature. Results show that most of the surface temperatures in downtown Beijing are distributed between 21 and 32 degrees Celsius in summer, demonstrating significant spatial variability, especially in the downtown area with higher temperature values, proving that the UHI effect is more significant in the residential areas. This finding validates the high-precision inversion capability of the single-window algorithm in complex urban environments. The study also suggests that the surface temperature inversion can be further improved by introducing more remote sensing data and improving the algorithm in the future.

Keywords: Landsat 8; Surface Temperature Inversion; Beijing; Remote Sensing; Urban Heat Island Effect.

1. Introduction

Land Surface Temperature (LST), as a key indicator in climatology, environmental science and urban thermal environment analysis, carries the important task of revealing the urban heat island (UHI) effect and global climate change trends and assisting in urban planning and environmental protection policy formulation [1,2]. The accurate acquisition and monitoring of LST is important for understanding the UHI effect, climate change, and the formulation of urban planning and environmental protection policies [3].

In recent years, with the continuous progress of remote sensing (RS) technology, using satellite RS to capture surface temperature information has become a mainstream practice in this field [4]. Recently, with the continuous progress of RS technology, utilizing satellite RS to capture surface temperature information has become a mainstream practice in this field. Among them, Landsat 8 satellite data have high spatial resolution and rich spectral information (1-7,9 - Operational Land Imager (OLI) multispectral band (30 m); 8 -OLI panchromatic band (15 m); 10,11 - Thermal Infrared Sensor (TIRS) band (30 m)), which have become an important source of data for surface temperature inversion studies.

The Landsat 8 satellite has a thermal infrared sensor (TIRS) capable of capturing thermal infrared radiation data in the 10.9-micron and 12.0-micron bands. The inverse calculation of surface temperature is limited by multiple factors such as atmospheric conditions, surface material composition, and thermal radiation properties, so exploring the use of Landsat 8 data to accurately derive surface temperature and effectively calibrate the results has become the focus and challenge of the current scientific research field.

Beijing, as China's capital city and megacity, is an ideal area for surface temperature inversion studies due to its complex geographic and climatic conditions and the significant UHI effect. Inversion and validation of surface temperature in Beijing not only help to reveal the spatial distribution

characteristics of its urban thermal environment but also provide a reference for environmental monitoring in other megacities. This study takes Beijing as an example and analyzes the surface temperature by using Landsat 8 satellite data, surface thermal radiation intensity calculation and single window algorithm inversion algorithm.

2. Background of Beijing City

Beijing, the capital of China, is located in the north of the Tropic of Cancer, and the climate type belongs to the continental monsoon climate, with an average annual temperature of 10-12 °C and an average annual precipitation of 644mm. The four seasons are clear: dry in winter, windy in spring, rainy in summer, and sunny and mild in fall. The terrain is mainly in the plains, with an average elevation of about 43.5m above sea level.

The central urban area of Beijing covers 16 administrative districts, such as Dongcheng, Xicheng, Haidian, Chaoyang, Fengtai, Mentougou, with a total area of 16,410 square kilometers (Figure 1). Through in-depth exploration of these areas, this study aims to comprehensively analyze the climatic characteristics, topography and landscape of Beijing and the related environmental challenges, to lay a solid scientific foundation for the city's future planning decisions and sustainable development.

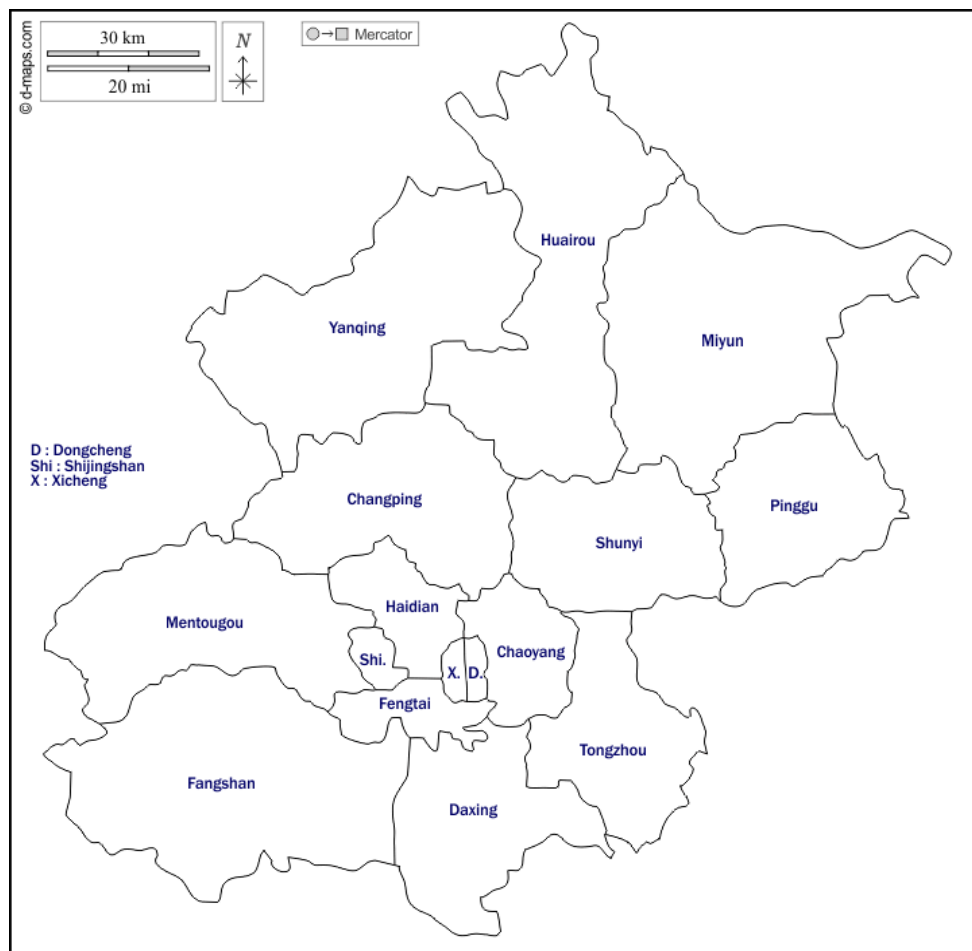


Figure 1. Regional map of Beijing city [5]

3. Research Data and Pre-Processing

3.1. Data Sources

RS imagery of downtown Beijing is selected from the Landsat series of satellites. Specifically, the Landsat 8 satellite has continued to operate since its successful launch in 2013, with a global coverage cycle of once every 16 days. The satellite has two key sensors: OLI and TIRS, which provide

information in 11 bands. Among them, the OLI segment covers 9 bands and achieves 15 m panchromatic resolution with 30 m multispectral resolution, while the TIRS provides 100 m spatial resolution and focuses on the thermal infrared band (Table 1). The Landsat8 data adopted in this study, involving the main orbit number 123/32, were taken in the summer of 2021, a period of low cloud cover and high image clarity, providing excellent conditions for accurate temperature inversion analysis [6].

In addition, this study uses data from the official platform of the National Aeronautics and Space Administration (NASA) to determine atmospheric transmittance. Based on core parameters such as the time of capture of each image and the geographic location of its center, this study obtained specific atmospheric transmittance values for the moment of capture of each image.

Table 1. Landsat8 sensor and band characteristics

Transducers	Wave Band	Wavelength Range/Mm	Resolution/m
OLI	1-Coastal/Aerosol	0.43-0.45	30
	2-Blue	0.45-0.51	30
	3-Green	0.53-0.59	30
	4-Red	0.64-0.67	30
	5-NIR	0.85-0.88	30
	6-SWIR1	1.57-1.65	30
	7-SWIR 2	2.11-2.29	30
	8-PAN	0.50-0.68	15
	9-Cirrus	1.36-1.38	30
TIRS	10-TIR	10.60-11.19	100
	11-TIR	11.50-12.51	100

3.2. Image Data Preprocessing

The image data mainly includes the image data covering the urban area of Beijing and the vector data of the administrative districts of Beijing.

In order to eliminate the interfering effects of atmospheric absorption, solar radiation, and terrain features on the images, a series of preprocessing operations such as radiometric calibration, atmospheric correction and cropping needs to be performed on the images (Figure 2). Radiometric calibration, as a key step in the preprocessing of RS images, focuses on converting physical quantities such as digital number, radiant brightness, and temperature, so that the subsequent quantitative analysis can be carried out smoothly. Atmospheric correction is a key step in the preprocessing of RS images [7]. It aims to correct image deviations caused by atmospheric water vapor, particles, etc.

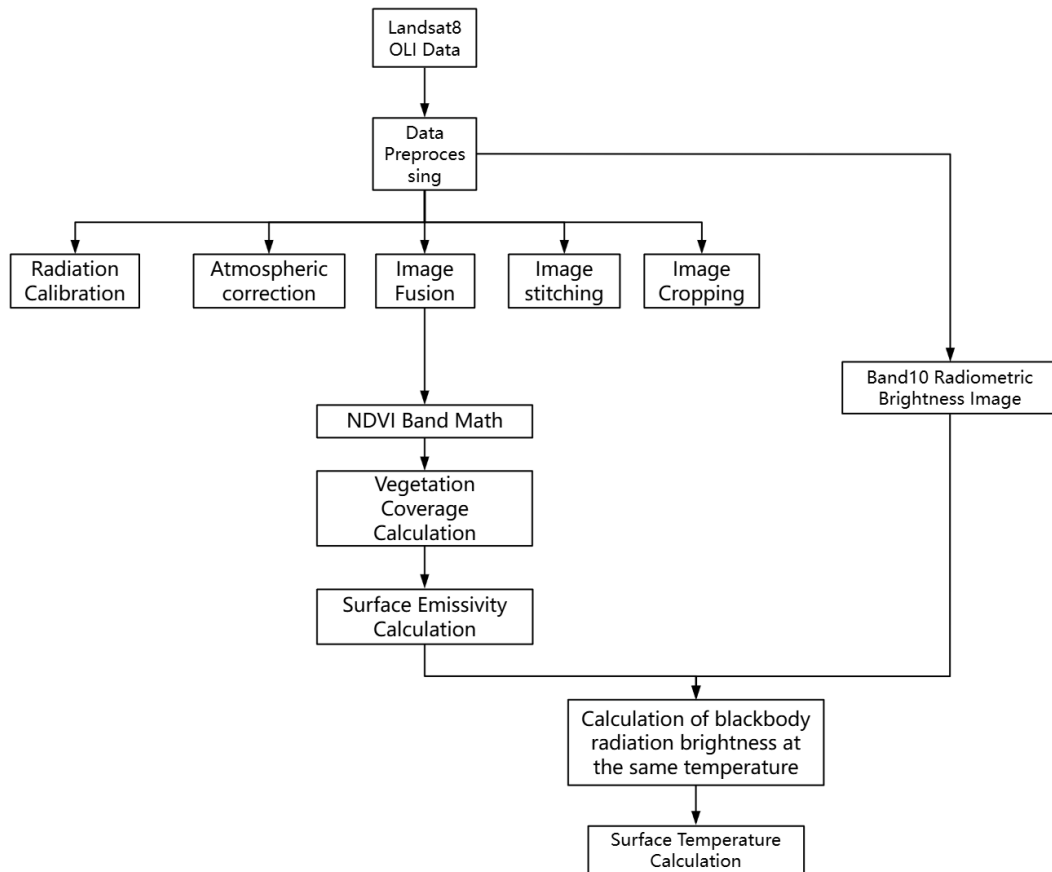


Figure 2. Flow chart of the study (Original Figure)

4. Research Methodology

The preprocessed data were used to calculate the Normalized Vegetation Index (NDVI) to assess the vegetation cover of the study area. This step further calculates the vegetation cover by inverting the NDVI and calculating surface-specific radiance. Then, the thermal infrared image of Band 10 was extracted, and the inversion of surface temperature was carried out using the single window algorithm through the parameters of surface-specific radiance, brightness temperature and atmospheric equivalent temperature. Finally, the surface temperature distribution map was calculated and derived, which provided the basic data for the thermal environment analysis of the study area (Fig. 2).

4.1. Surface Specific Emissivity

4.1.1. Normalized Vegetation Index inversion.

The NDVI index measures the ratio of the difference in reflectance between the near-infrared and red-light bands in remotely sensed imagery to its sum. It is effective in assessing vegetation growth and cover, correcting for radiometric errors to a certain extent, and revealing the potential influence of the plant canopy on the results of the observations. NDVI ranges between -1 and 1. Negative values indicate surface cover with high visible light reflectances, such as clouds, water, or snow. Zero corresponds to rocky or bare soil surfaces, where the reflectance intensity of near-infrared light is similar to that of red light. Positive values imply the presence of vegetation, and are positively correlated with the density of vegetation. For instance, the more luxurious vegetation has higher NDVI values. Especially at low and medium levels of vegetation cover, the NDVI value increases significantly with the increase of cover until it reaches a certain saturation point, at which point the growth rate slows down. Therefore, NDVI is suitable index in monitoring the growth dynamics of vegetation in the early to middle stage. The following formula calculates NDVI [8]:

$$NDVI = (NIR - R)/(NIR + R) \quad (1)$$

Where R is the reflectance value in the red band.

4.1.2. Vegetation cover.

The calculation of the NDVI determines the degree of vegetation cover in the study area. The following formula usually calculates vegetation cover (Pv) [9]:

$$P_v = \left(\frac{NDVI - NDVI_{min}}{NDVI_{max} - NDVI_{min}} \right)^2 \quad (2)$$

Where NDVImin and NDVImax are the minimum and maximum values of NDVI, respectively.

4.1.3. Surface-specific emissivity.

The specific emissivity of an object refers its ability to emit electromagnetic waves outward, and it reflects the proportionality between the intensity of radiation emitted from the surface and from an ideal blackbody under the same temperature. In this study, the NDVI threshold method proposed by Sobrino was used [9]:

$$\varepsilon = 0.004P_v + 0.986 \quad (3)$$

Where 0.004 is an empirical coefficient, and 0.986 is the base value of radiance when vegetation is fully covered.

4.2. Radiant Brightness Temperature

4.2.1. Radiant brightness values.

According to the radiative transfer equation formulation, a blackbody with temperature labeled T exhibits a radiant brightness B(T_s) in the thermal infrared band, which can be exhaustively expressed by the following equation:

$$B(T_s) = [L_\lambda - L_\mu - \tau - (1 - \varepsilon)L_d]/(\tau - \varepsilon) \quad (4)$$

Where T_s indicates the actual temperature of the surface; L_λ represents the brightness of thermal infrared radiation, which is related to the wavelength λ corresponding to the thermal radiant brightness of the blackbody determined according to Planck's law at T_s; L represents the level of radiant brightness upward in the atmosphere; τ demonstrates the transmittance of the atmosphere in the thermal infrared band; ε indicates the radiance of the surface; L_u and L_d represent the upward and downward radiant brightness level of the atmosphere, respectively.

4.2.2. Radiant brightness temperature.

Based on the inverse function of Planck's formula, it is the radiant brightness temperature (Ti) that is found to be [10].

$$Ti = \frac{K_2}{\ln\left[\frac{K_1}{B(T_s)} + 1\right]} - 273 \quad (5)$$

Where the values of K1 and K2 correspond to the TIRS Band10 data, which are 774.89 W/(m²-μm-sr) and 1321.08 K, respectively.

4.3. Surface temperature inversion

The true inversion temperature at the surface (T_s) can be calculated by a single-window algorithm with the following equation:

$$T_s = \{-76.35(1 - C - D) + [0.458(1 - C - D) + C + D] * T_b - D * T_a\} / C \quad (6)$$

T_s is closely related to the surface brightness temperature detected in the thermal infrared band (T_b), and the atmospheric equivalent temperature (T_a).

The nature of the atmospheric equivalent temperature depends on the state of the temperature distribution in the atmosphere and the specific conditions of the atmosphere; it is worth noting that under typical atmospheric modeling, there is a linear correlation pattern between T_a and the temperature close to the surface, which is defined as the temperature at a height of 2 meters above the surface (T_0). There exists a linear correlation pattern. To date, several researchers in the national academic community have explored the details of this particular linear relationship in depth and have proposed various mathematical formulas to express the correlation. Two empirically determined constants based on -67.355351 and 0.458606 are introduced in the formula for T_s , while C and D are intermediate variables in this calculation process, and their respective calculation rules follow the derivation of the following equations.

$$C = \varepsilon * \tau \quad (7)$$

$$D = (1 - \tau) * [1 + (1 - \varepsilon) * \tau] \quad (8)$$

5. Results and Discussion

5.1. Surface Temperature Inversion Results

According to the relevant statistics, during June 2021, the temperature range in the urban center of Beijing was maintained between 21 and 32 degrees Celsius. Through inverse analysis using Landsat8 data, the surface temperature distribution map of urban areas in Beijing is obtained (Figs. 3,4). The results show that 80% of the frequency distribution of the surface temperature in the urban area of Beijing is concentrated in the above temperature range, which is an important reference value for related research.

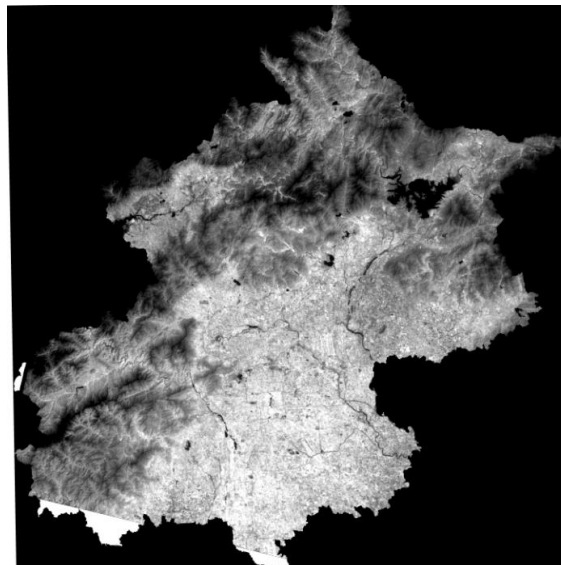


Figure 3. Temperature inversion diagram (Original Figure)

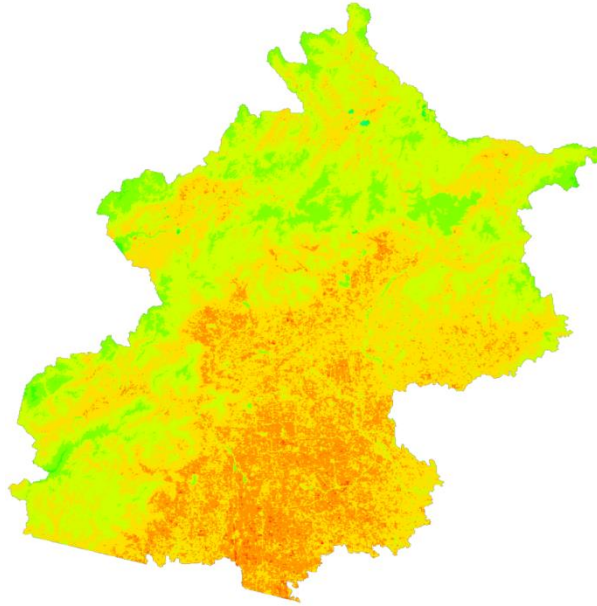


Figure 4. Temperature classification diagram (Original Figure)

5.2. Discussion

The results of surface temperature inversion using the single window algorithm show a high degree of consistency between the estimated and measured values, which verifies the high reliability and accuracy of the algorithm in the surface temperature inversion task. In particular, the algorithm can produce accurate temperature measurements when facing complex and changing surface conditions in urban environments, further emphasizing its applicability and accuracy under complex conditions.

According to the temperature inversion map and the temperature distribution map, the surface temperature in Beijing shows significant spatial variability. Higher temperatures are recorded in the center of the city, while the suburban fringes and green areas show relatively lower temperatures. The city center area shows a more significant temperature increase than its surrounding areas. This phenomenon strongly suggests the profound influence of urbanization and human activities on surface temperature, especially in built-up areas and industrialized parks, where the sharp increase in surface temperature cannot be ignored.

Surface temperature inversion results are indispensable for urban planning and environmental protection. By scrutinizing the distribution patterns of surface temperatures, it is possible to identify areas of concentration of the UHI effect and adopt targeted mitigation strategies, such as expanding the coverage of the green regions and improving the spatial layout of cities. In addition, these inversions are essential for developing a more rigorous model for managing the urban thermal environment, which will help mitigate the possible adverse effects of hot climatic conditions on the health of citizens.

The methodology adopted and the results obtained in this study have laid a solid foundation for subsequent investigations of surface temperature inversion. Nevertheless, there is still room for improvement and optimization. For example, more diversified RS data types, such as hyperspectral data and radar data, and more sophisticated inversion calculation strategies, such as multi-window algorithms, can be considered to improve the accuracy of the inversion. In addition, a deeper exploration of the superimposed effects of different surface characteristics, climatic conditions and anthropogenic activities on surface temperature is needed to present more comprehensive images.

6. Conclusion

In this study, Landsat 8 data resources and single-window algorithms were successfully applied to realize the high-precision inversion of the surface temperature of Beijing, and the validation confirmed the validity of the method.

The study confirms the high reliability and accuracy of the single window algorithm for surface temperature inversion, particularly in complex urban environments. The spatial variability of surface temperatures in Beijing, with higher temperatures concentrated in the downtown area and lower temperatures in suburban and green areas, underscores the significant impact of urbanization on the urban thermal environment. These findings highlight the importance of surface temperature inversion in urban planning and environmental protection, suggesting that targeted strategies, such as increasing green space and optimizing urban layouts, can decrease the UHI effect.

These results are valuable for analyzing the spatial distribution characteristics of the urban thermal environment and also provide a strong basis for promoting the science of urban planning and the effectiveness of environmental protection. Future research should focus on integrating diverse RS data and advanced inversion techniques to further enhance the accuracy and comprehensiveness of urban thermal environment assessments.

References

- [1] LI Zhiqian, Gong Cailan, HU Yong, Yin Qiu and Kuang, Dingbo. The Progress of the Remote Sensing Research on Urban Heat Island. 2009.
- [2] Zhang Aiyin, Zhang Xiaoli. Land surface temperature retrieved from Landsat-8 and comparison with MODIS temperature product. *Journal of Beijing Forestry University*, 2019, 41 (3): 1 - 13. DOI: 10.13332/j.1000 - 1522.20180234.
- [3] LI Yuanzheng, YIN Ke, ZHOU Hongxuan, WANG Xiaolin, HU Dan. Progress in urban heat island monitoring by remote sensing. *PROGRESS IN GEOGRAPHY*, 2016, 35 (9): 1062 - 1074 <https://doi.org/10.18306/dlkxjz.2016.09.002>.
- [4] Duan SB, Ru C, Li ZL, et al. Reviews of methods for land surface temperature retrieval from Landsat thermal infrared data. *National Remote Sensing Bulletin*, 2021, 25 (8): 1591 - 1617 DOI: 10.11834/jrs.20211296.
- [5] Beijing free map, free blank map, free outline map, free base map outline, prefectures, names, white. https://d-maps.com/carte.php?num_car=21507&lang=en.
- [6] MA Lingling, WANG Ning, GAO Caixia, ZHAO Yongguang, YANG Benyong, WANG Xinhong, HAN Qijin, XU Na, SONG Peilan, LIU Yaokai. XXXX. On-orbit absolute radiometric calibration for optical remote sensing satellites: progress and trends. *National Remote Sensing Bulletin*, 2023, 27 (5): 1061 - 87.
- [7] Herbei MV, Sala F, Boldea M. Relation of normalized difference vegetation index with some spectral bands of satellite images. In *AIP Conference Proceedings*. 2015, 1648 (1).
- [8] SOBRINA J A, JIMENEZ-MUNOZ J C, PAOLINI L. Land surface temperature retrieval from Landsat TM 5. *Remote Sensing of Environment*, 2004, 90: 434 - 440.
- [9] Callejas IJ, de Oliveira AS, de Moura Santos FM, Durante LC, de Jesus Albuquerque Nogueira MC, Zeilhofer P. Relationship between land use/cover and surface temperatures in the urban agglomeration of Cuiabá-Várzea Grande, Central Brazil. *Journal of Applied Remote Sensing*. 2011, 5 (1): 053569.
- [10] Hao X, Qu JJ, Hauss B, Wang C. A high-performance approach for brightness temperature inversion. *International Journal of Remote Sensing*. 2007, 28 (21): 4733 - 43.